

CUMULATION AND SPALLATION WITH LOCAL THERMAL SHOCKS  
IN METALS DISKS

É. I. Andriankin, V. A. Andrushchenko,  
and N. N. Kholin

UDC 539.42:620.172.254:539.14

The contribution of two mechanisms of cumulation to the process of spallation of metal disks is studied numerically. The dimensions of the spallation zones are estimated and their location is determined as a function of the plastic and viscous properties of the material.

The fact that waves of unloading build upon the axis of symmetry of an instantaneously heated cylinder was established in 1965-1966 (see [1, 2]). A more detailed investigation [3] showed that when the temperature in an infinite elastic isotropic cylinder with a free side surface is raised suddenly, transverse thermoelastic waves of unloading, moving toward the axis of symmetry, form. Their intensity grows in proportion to  $r^{-1/2}$  and at the moment of arrival at the axis the amplitude of the waves of unloading becomes infinite. Such cumulation also occurs in real media, but the intensity of the waves collapsing on the axis of the cylinder is, naturally, finite.

In [4] cumulation of waves of compression was observed in an investigation of the process of wave formation under an axisymmetric thermal shock in disks (in a hydrodynamic formulation). The secondary shock wave, which is much stronger than the primary shock wave (initiated by the initial heating), formed in the process propagates along the axis of symmetry toward the free end (or ends in the case of internal heating) and, reflected from it (them), propagates along the medium as a longitudinal rarefaction wave. The calculations performed in [5, 6] for a solid deformed body confirmed these results.

Thus both cumulation mechanisms described above ultimately lead to the appearance of strong tensile stresses in the vicinity of the axis of symmetry and in many cases they are strong enough to produce spallation.

1. The starting system of equations describing the motion of an elastic medium for velocities and strains in a two-dimensional axisymmetric case have the form

$$\frac{\partial p}{\partial t} = -(np + 1) \operatorname{div} \mathbf{v}, \quad (1)$$

$$\frac{\partial u}{\partial t} = -\frac{\partial p}{\partial r} + \frac{\partial S_r}{\partial r} + \frac{\partial \tau}{\partial z} + \frac{S_r - S_\varphi}{r}, \quad (2)$$

$$\frac{\partial v}{\partial t} = -\frac{\partial p}{\partial z} + \frac{\partial S_z}{\partial z} + \frac{\partial \tau}{\partial r} + \frac{\tau}{r}, \quad (3)$$

$$\frac{\partial S_r}{\partial t} = 2c^2 \left( \frac{\partial u}{\partial r} - \frac{1}{3} \operatorname{div} \mathbf{v} \right), \quad (4)$$

$$\frac{\partial S_z}{\partial t} = 2c^2 \left( \frac{\partial v}{\partial z} - \frac{1}{3} \operatorname{div} \mathbf{v} \right), \quad (5)$$

$$\frac{\partial S_{\phi}}{\partial t} = 2c^2 \left( \frac{u}{r} - \frac{1}{3} \operatorname{div} \mathbf{v} \right), \quad (6)$$

$$\frac{\partial \tau}{\partial t} = c^2 \left( \frac{\partial v}{\partial r} + \frac{\partial u}{\partial z} \right). \quad (7)$$

Here the equation for the pressure  $p$  (1) ( $0 \leq r \leq R$ ,  $0 \leq z \leq H$ ) is written using the equation of state  $p = (\rho^n - 1)/n$  instead of the equation of continuity.

In the case when the viscous properties of the material are taken into account terms of the form  $c^2 \operatorname{Re} S_i / \mu$  and  $c^2 \operatorname{Re} \tau / 2\mu$  are added on the right sides of the equations for the deviator  $S_i$  and the tangential stress  $\tau$  (4-7).

For elastoplastic materials the plasticity is introduced as follows. In the entire region of motion of the medium Mies' creep condition  $S_r^2 + S_z^2 + S_{\phi}^2 + 2\tau^2 \leq 2/3Y^2$  is checked. This relation means that the intensity of the stresses cannot exceed the dynamic yield stress of the material  $Y$ . If the excess change in the stresses at some point in the medium results in this inequality being violated, then each element of the deviator  $S_i$  and  $\tau$  are multiplied by a correction factor  $\sqrt{2/3Y} / \sqrt{S_r^2 + S_z^2 + S_{\phi}^2 + 2\tau^2}$ . This reduction of the stresses, perpendicular to the circle of creep, affects only the plastic part of the stresses and is equivalent (as shown by S. S. Grigoryan) to the use of the Prandtl-Rice equations for plastic flow.

The boundary and initial conditions are presented below for specific problems.

2. The system of differential equations (1)-(7) can be approximated by a difference system using an explicit difference scheme of the type predictor-corrector-"leap-frog" [7]. An explicit method was chosen because the program was implemented on a computer with a vector processor (MAMO ES-1055M matrix module) and explicit schemes are structurally more amenable to parallel formulation than are implicit schemes, that they are better adapted to the architecture of such machines. In addition the advantages gained by vectorization of the algorithm and the program significantly compensate for the time losses associated with the stringent restriction on the step size for integration over time (Courant's conditions). Thus the use of a matrix module for vectorization of the algorithm and the program reduces the computing time of a variant by a factor of 5-9 (depending on the number of points in the working grid).

The "leap-frog" scheme, in the case when the intermediate layer is chosen to be at the center ( $\lambda = 1/2$ , see [7]), has second-order accuracy, but as V. N. Kukudzhaynov showed [8] taking plasticity into account using the procedure of reduction on the circle of creep lowers the order of the approximation, since the "correction" itself, without rescaling corresponds to a difference scheme with first-order accuracy.

Two approaches are employed for numerical integration of systems of hyperbolic equations. In the first approach singularities are singled out, while the second approach is a through approach. The method of singling out singularities (shock waves, contact surfaces, etc.) is usually employed when the number of discontinuities is small, otherwise the computing algorithm becomes extremely complicated. In dynamic multidimensional problems in the theory of elasticity (and elastoplasticity), however, the number of discontinuities is large and increases rapidly as a result of the reflection of waves from boundaries and interaction with one another. For this reason the through method of computation is more efficient for solving these problems. The main drawback of this method is that nonphysical oscillations arise in the vicinity of discontinuities. To damp these extraneous oscillations and to intensify the stabilizing properties of the scheme a smoothing operator of the Book-Boris monotimizer type, proposed in [9], is employed.

3. One of the most efficient methods for checking the accuracy of the solution and finding possible errors in the program at the debugging stage is compare with the exact solution the results of the numerical solution of a problem that can be solved analytically.

For problems in mathematical physics the existence of such a test is extremely rare and for this reason it is of great value to anyone performing computations. Here we were able to find such a formulation to test the numerical procedure, the algorithm, and the program. In addition, the efficiency of the matrix module was checked for the same test problem.

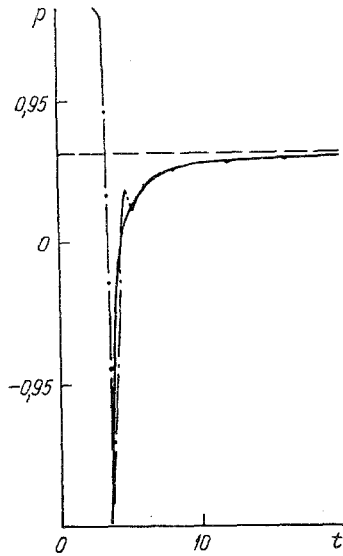


Fig. 1

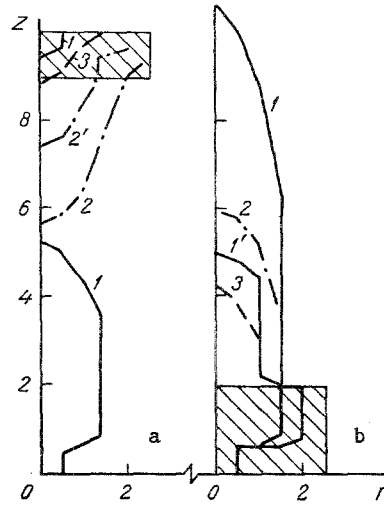


Fig. 2

Fig. 1. The time dependence of the pressure  $p(t)$  at points on the symmetry axis.  $p$ , GPa;  $t$ ,  $\mu\text{sec}$ .

Fig. 2. The boundaries of the regions of spallation of the material under a local thermal shock: a) at the center of the disk, b) at the end.  $z$ ,  $r$ , mm.

So, we are solving the problem of cumulation of waves of unloading. This problem has an analytical solution [2]. Let a constant stress appear initially (for example, as a result of instantaneous heating) in an infinite cylindrical region with radius  $R_1$  in a linearly elastic ( $\nu = 1$ ) isotropic medium. Then the starting wave equation has an exact solution on the symmetry axis of the cylinder [2]. For example, for the pressure this solution has the form

$$p(t) = p_0 \text{ for } t < \frac{R_1}{c_1},$$

$$p(t) = \frac{p_0}{3} \frac{1-2\nu}{1-\nu} \left[ 2 + \frac{\nu+1}{1-2\nu} \left( 1 - \frac{1}{\sqrt{1 - \left(\frac{R_1}{c_1 t}\right)^2}} \right) \right]$$

$$\text{for } t > \frac{R_1}{c_1},$$

where  $p_0$  is the initial pressure.

As  $t \rightarrow \infty$  the pressure approaches the static solution:

$$p_1 = \lim_{t \rightarrow \infty} p(t) = \frac{2}{3} p_0 \frac{1-2\nu}{1-\nu}.$$

The same problem was solved numerically using the method described above. In Fig. 1 the exact solution (solid curve) is compared with the numerical solution (dot-dashed curve). As the calculations showed, the solutions  $P(t)$  differ only in the vicinity of the singular point of the exact solution ( $t = R_1/c_1$ ); this is understandable, since owing to some smoothing in the initial conditions and the existence of grid viscosity the numerical solution does not have a singularity.

In addition, the solution for the intensity of waves of unloading at the stage of the initial collapse was checked. As established in [3], the increment to the amplitude in the jumps of rarefaction  $\Delta p$  is proportional to  $r^{-1/2}$ .

TABLE 1. Check of the Law of Increase of the Amplitude

$r/R_1$	$\sqrt{r/R_1}$	$p$ , GPa	$\Delta p$ , GPa	$\Delta p/\Delta p_1$	$(r/r_1)^{-1/2}$	% deviation
0,9	0,9487	0,8371	0,7724	—	—	—
0,75	0,866	0,7558	0,8537	1,105	1,095	0,91
0,6	0,7746	0,6531	0,9564	1,238	1,225	1,06
0,45	0,67082	0,51264	1,06989	1,42	1,414	0,45
0,3	0,54772	0,27193	1,33760	1,7317	1,732	0,02
0,15	0,3873	-0,40724	2,01677	2,611	2,45	6,57
0,1	0,31623	-0,41061	2,02014	2,615	3	12,8

In the table  $r/R_1$  are the values of the relative coordinate of the wave of unloading,  $p$  is the amplitude of the wave,  $\Delta$  is the increment of the amplitude compared with the initial value 1.60953 GPa,  $\Delta p/\Delta p_1$  is the ratio of the increment to the intensity of the wave for different values of the radii  $r/R_1$  and the increment at  $r_1/R_1 = 0.9$ ,  $(r/r_1)^{-1/2}$  is the coordinates to the power  $-1/2$ , and the relative deviation in percent from the ratio  $\Delta p/\Delta p_1 = (r/r_1)^{-1/2}$  is given in the last column.

As one can see from Table 1, for radii  $r/R_1 \geq 0.3$  the indicated ratio holds to within 1%, for  $r/R_1 = 0.15$  the deviation is equal to 6.57%, and for  $r/R_1 = 0.1$  the deviation is equal to 12.8%. These deviations occur for the same reasons: the starting "smearing" of the wave and the grid viscosity.

The calculation of this test problem in order to determine the speed up of the calculation with the use of the vector processor was performed on grids with  $37 \times 51$ ,  $76 \times 101$ , and  $151 \times 201$  nodes. The obtained results of the comparison of the computing times for these variants using programs employing and not employing a matrix module are as follows: the speed up factor is equal to about 2 on the  $37 \times 51$  grid, 6.7 on the  $76 \times 101$  grid, and 9.2 on the  $151 \times 201$  grid. The maximum speed up of the calculation was obtained, naturally, with the larger number of nodes; this indicates that the matrix module is highly efficient for complex problems, in which a numerical investigation is possible only on detailed grids.

4. We are studying the problem of wave formation, growth in damage, and development of spallation zones in metal disks under a thermal shock. The thermal shock is produced by instantaneous heating of the local cylindrical zones, coaxial with the disk, at the surface of the disk, or in the disk. In the first case the physical process of heating of the surface with a laser pulse is modeled and in the second case an internal zone is heated with a electron beam.

This physical problem can be formulated mathematically as follows: find the functions  $\mathbf{v}$ ,  $p$ ,  $S_i$ ,  $\tau$  in the region  $G(0 \leq r \leq R, 0 \leq z \leq H)$ , which satisfy the system of equations (1)-(7) and the initial conditions

$$\begin{aligned} \mathbf{v} = S_i = \tau = 0 \text{ in the region } G, \quad p = 0 \text{ in } G/G_0, \\ p = p_0 > 0 \text{ in } G_0 (0 \leq r \leq r_1, h_1 \leq z \leq h_2) \end{aligned} \quad (8)$$

and the boundary conditions

$$\begin{aligned} S_r = p = \tau = 0 \quad \text{if} \quad r = R, \quad 0 \leq z \leq H, \\ S_z = p = \tau = 0 \quad \text{if} \quad \begin{cases} z = 0, \quad 0 \leq r \leq R, \\ z = H, \quad 0 \leq r \leq R, \end{cases} \\ u = \tau = 0 \quad \text{if} \quad r = 0, \quad 0 \leq z \leq H. \end{aligned} \quad (9)$$

The problem (1)-(9) formulated above was solved for aluminum disks with the following values of the parameters:  $R = 2.5 \cdot 10^{-2}$  m,  $H = 2 \times 10^{-2}$  m,  $C_1 = 5500$  m/sec,  $\rho = 2700$  kg/m<sup>2</sup>,  $n = 3.5$  (i.e., the spherical part of the stress tensor depends nonlinearly on the density,  $n \neq 1$ ). We studied the elastic ( $Y \rightarrow \infty$ ,  $Re = 0$ ), elastoplastic ( $Y = 0.12$  GPa,  $Re = 0$ ), and elastoviscous ( $Y \rightarrow \infty$ ,  $Re = 70$ ) models of the disk material.

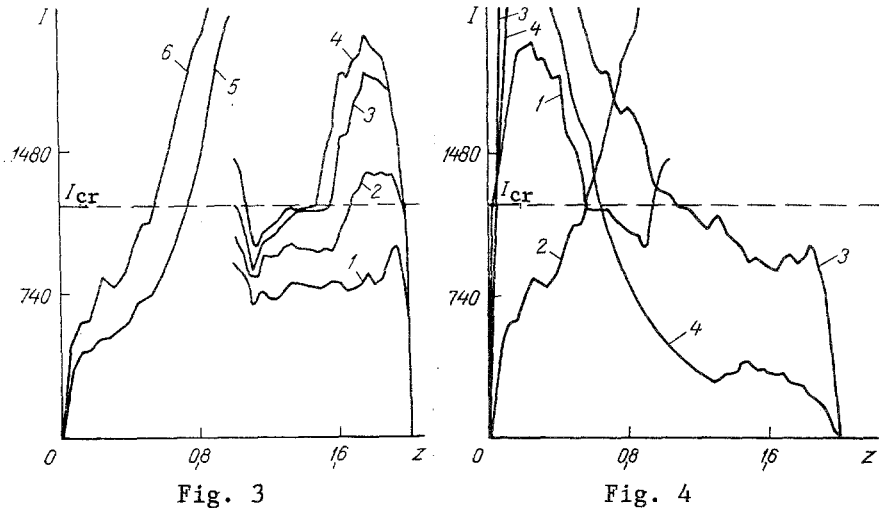


Fig. 3. The distribution of integrals of damage  $I(z)$  along the axis of symmetry with a local thermal shock at the center of the disk for different times (curves 1-4 are for an elastic material and curves 5-6 are for an elastoplastic material).  $I$ , Pa·sec,  $z$ , cm.

Fig. 4. The final distributions of the integrals of damage  $I(z)$  along the axis of symmetry with a thermal shock at the center of the disk and at the ends for different mechanical properties of the material.

The zone of heating  $G_0$  is chosen to be small compared with the region  $G$ :  $[0, r_1] = 2.5 \cdot 10^{-3}$  m,  $[h_1, h_2] = 2 \cdot 10^{-3}$  m; in the first case it lies on the surface of the disk and in the second case it lies in an interior region at the same distance from both ends. The starting pressure produced by the heating is  $p_0 = 5$  GPa.

Investigation of the spallation of bodies is connected with establishing an adequate criterion for fracture. In this work, in modeling the process of dynamic fracture numerically we employed the continuum theory of damage. The criterion of fracture in this case is a damage integral of the following form [4]:

$$I = \int_0^t |p| \exp [-(|p| - p_1)/p_2] d\tau. \quad (10)$$

Physically this criterion corresponds to taking micropores into account in the waves of unloading and the growth of these pores to some critical value  $I_{cr}$  (for aluminum  $I_{cr} = 1220$  Pa·sec). We note that the summation in Eq. (10) is performed for  $p < p_1$  and  $|p| > p_1$  (here  $p_1 = 0.176$  GPa,  $p_2 = 0.21$  GPa).

5. We shall now discuss the results. First we shall study the case of a thermal shock in a local region at the geometric center of the disk. A strong electromagnetic pulse produces practically instantaneous ( $t \leq 10^{-8}$  sec) heating of a cylindrical region. Initially a wave of unloading and a wave of compression start to move, respectively, toward the axis of symmetry and toward the side surface from the side boundary of this zone. Like in the case studied in Sec. 3 as the waves approach the axis of symmetry (by the time  $t = 0.45-0.5$   $\mu$ sec) the amplitude of the waves of unloading increases rapidly, reaching values of 3-4 GPa in modulus, much higher than  $p_1 = 0.175$  GPa in the formula (10). As a result of this damage starts to accumulate in the vicinity of the symmetry axis near the zone of the thermal shock. The process of collapse and reflection of waves of unloading from the axis lasts much longer in an elastoplastic medium than in an elastic medium, because the velocity of propagation of the elastoplastic wave is lower and therefore the process of damage cumulation lasts longer. This time interval is sufficient for the integral (10) to reach a critical value in a relatively large zone in a neighborhood of the  $Oz$  axis in a disk of elastoplastic material, i.e., approximately by the moment 3.3  $\mu$ sec spallation of the material occurs in a region encompassing the zone of heating and a cavern forms. In Fig. 2, where the lower half of the plane of the section  $rOz$  is shown, the curve 2' indicates the lower boundary of the region of spallation as a result of the action of the first mechanism of cumulation in the elastoplastic case.

up to the moment  $t = 3.3 \mu\text{sec}$  (the cross-hatched rectangle at the top of the figure is the bottom half of the zone of heating). The process of spallation occurs analogously, but less intensively, in an elastoviscous material (see curve 3 in Fig. 2a). Since the distances over which this process occurs are short (of the order of millimeters) the dissipation of energy owing to viscosity is negligible. The viscosity has virtually no effect on the amplitude of the waves of unloading, but it nonetheless "stretches out" the characteristic time of reflection as compared with the case of an elastic material and therefore the damage cumulation time. In an elastic medium, however, where the arrival of the wave of unloading at the Oz axis and its reflection occur more rapidly, there is not enough time for integral (10) to reach the critical value (see curve 1 in Fig. 3, which shows the distribution  $I(z)$  along the axis of symmetry for  $t = 5.7 \mu\text{sec}$ ) and spallation does not occur. The figure shows only half of the graphs, since they are symmetric relative to the central section.

Further development of the wave-formation process occurs as follows. Some time after the reflection of the wave of unloading a secondary cumulation shock wave is generated in a zone near the axis of symmetry; the amplitude of this shock wave is much higher than the amplitude of the primary wave, initiated by the initial heating. A compression wave generated by cumulation moves toward the free ends of the disk and is reflected from them by intense waves of unloading. In an elastic material the amplitude of these waves is greater than  $p_1$ , while in elastoplastic and elastoviscous materials it is less than  $p_1$ . Thus, as the waves of unloading move away from the free ends of the disk toward the center in the first case spallation occurs (see curves 2, 3, and 4 in Fig. 3, corresponding to the times 14, 24, and 33  $\mu\text{sec}$ ), while in the other cases the spallation does not occur.

Further, an accompanying collision of these waves of rarefaction occurs in the central section of the disk; as a result of this collision more intense waves of unloading, propagating toward the ends, are formed. In an elastic material they result in the formation of a spallation zone in the central region and in some increase of the zones of spallation at the faces (see curve 1 in Fig. 4 ( $t = 33 \mu\text{sec}$ ) as well as curve 1 in Fig. 2a). In an elastoplastic medium in medium intense diverging waves of unloading significantly increase the volume of the spallation cavern (compare curves 5 ( $t = 5.7 \mu\text{sec}$ ) and 6 ( $t = 3 \mu\text{sec}$ ) in Fig. 3 and curves 2' and 2 in Fig. 2a). Additional fracture does not occur only in the elastoviscous medium (the spallation zone remains bounded by the curve 3 in Fig. 2a). This confirms the results of previous studies [5], showing that at distances of the order of centimeters in viscous media dissipation significantly weakens the wave processes.

Thus the numerical experiment shows that under conditions of a thermal shock in a local central zone the cumulation effect as a result of collapse of transverse waves of unloading in an elastoplastic and elastoviscous media results in spallation of the material near the region of heating. In addition, in the latter case, the damage process is limited to this. In elastic media longitudinal waves of unloading, formed as a result of reflection of a secondary compression wave generated in the accumulation process, from the faces make the main contribution to the damage in the material. They more than double the volume of the spallation crater in an elastoplastic medium. In addition, and what is most interesting, in a "purely" elastic medium the thermal shock in a local zone around the center results primarily in endface spallation.

Next we study a thermal shock at the front face. In all three materials at the earliest stage (up to the moment  $t = 2 \mu\text{sec}$ ) spallation at the front face occurs as a result of the collapse of the side waves of unloading and the action of the rarefaction wave from the front face (see curves 1, 2, 3 in Fig. 2b; the cross-hatched rectangle is the zone of heating). For elastoviscous and elastoplastic media the damage process ends here. For an elastic material the spallation zone at this stage is smaller than for an elastoplastic material (compare curves 1' and 2 in Fig. 2b) because the collapse is more rapid, but in contradistinction to the case of heating of the central zone it nonetheless occurs. This is explained by the action of the additional wave of unloading from the front face.

Next, the wave formation and damage processes occur analogously to the case studied. In an elastic material a secondary wave with quite large amplitude is formed; the wave is reflected from the back face by an intense longitudinal wave of unloading. It leads to additional damage to the medium at the front face, thereby significantly increasing the volume of the spallation crater (compare curves 1' and 1 in Fig. 2b and curves 3 and 4 in Fig. 4).

Analysis of the computational results shows that in the case of heating of a local zone at the end of an elastic disk the cumulation of a secondary longitudinal wave of compression

makes the main contribution to the process of spallation damage, while in elastoplastic and elastoviscous materials all damage occurs with cumulation of transverse waves of unloading.

#### NOTATION

$t$ , time;  $r, z$ , cylindrical coordinates;  $\mathbf{v} = (u, v)$ , velocity;  $\rho$ ; density;  $p$ , pressure;  $S_i$ , components of the deviator of the stresses;  $\tau$ , tangential stress;  $n$ , constant in the equation of state;  $c_1$  and  $c_2$ , longitudinal and transverse velocities of sound;  $c = c_1/c_2$ ;  $\mu$ , coefficient of dynamic viscosity;  $Y$  is dynamic yield stress of the material;  $\nu$ , Poisson's ratio;  $Re$ , Reynolds number;  $R$  and  $H$ , radius and height of the disk;  $r_1$  and  $h$ , radius and height of the heated region;  $G$ , computing region;  $G_0$ , region of heating;  $\lambda$ , coefficient in the difference scheme.

#### LITERATURE CITED

1. J. J. Gilman and R. Bullough, Bull. Am. Phys. Soc., 10, No. 3, 334 (1965).
2. V. L. Indenbom and E. M. Shefter, Pis'ma Zh. Tekh. Fiz., 4, No. 7, 258-262 (1966).
3. V. I. Aleksandrovich and E. M. Shefter, "Some questions regarding the mechanics of deformable media," Moscow (1979); VINITI, No. 2235, June 21, 1979, pp. 21-27.
4. E. I. Andriankin, V. A. Andrushchenko, N. N. Kholin, and T. Z. Osmanov, "Laser-induced cumulation in a solid deformable body," Moscow (1986); VINITI, No. 3857, May 29, 1986, pp. 1-17.
5. E. I. Andriankin, V. A. Andrushechenko, and N. N. Kholin, Zh. Vychisl. Mat. Fiz., 27, No. 8, 1203-1211 (1987).
6. V. N. Aptukov and A. A. Pozdeev, Dokl. Akad. Nauk SSSR, 286, No. 1, 103-106 (1986).
7. Kh. S. Kestenboim, G. S. Roslyakov, and L. A. Chudov, Point Explosion. Computational Methods, Tables [in Russian], Moscow (1974).
8. V. N. Kukudzhanov, Numerical Methods for Solving Problems in the Theory of Elasticity and Plasticity [in Russian], Novosibirsk (1980), pp. 105-120.
9. A. I. Zhmakin and A. A. Fursenko, Zh. Vychisl. Mat. Mat. Fiz., 20, No. 4, 1021-1031 (1980).